The Astrophysical Journal, 713:584–591, 2010 April 10 doi:10.1088/0004-637X/713/1/584

AMiBA: SUNYAEV–ZEL'DOVICH EFFECT-DERIVED PROPERTIES AND SCALING RELATIONS OF MASSIVE GALAXY CLUSTERS

Yu-Wei Liao[1,2], Jiun-Huei Proty Wu[1], Paul T. P. Ho[2,3], Chih-Wei Locutus Huang[1], Patrick M. Koch[2], Kai-Yang Lin[1,2], Guo-Chin Liu[2,4], Sandor M. Molnar[2], Hiroaki Nishioka[2], Keiichi Umetsu[2], Fu-Cheng Wang[1], Pablo Altamirano[2], Mark Birkinshaw[5], Chia-Hao Chang[2], Shu-Hao Chang[2], Su-Wei Chang[2], Ming-Tang Chen[2], Tzihong Chiueh[1], Chih-Chiang Han[2], Yau-De Huang[2], Yuh-Jing Hwang[2], Homin Jiang[2], Michael Kesteven[6], Derek Y. Kubo[2], Chao-Te Li[2], Pierre Martin-Cocher[2], Peter Oshiro[2], Philippe Raffin[2], Tashun Wei[2], and Warwick Wilson[6]
[1] Department of Physics, Institute of Astrophysics & Center for Theoretical Sciences, National Taiwan University, Taipei 10617, Taiwan
[2] Institute of Astronomy and Astrophysics, Academia Sinica, P.O. Box 23-141, Taipei 10617, Taiwan
[3] Harvard-Smithsonian Center for Astrophysics, 60 Garden Street, Cambridge, MA 02138, USA
[4] Department of Physics, Tamkang University, 251-37 Tamsui, Taipei County, Taiwan
[5] University of Bristol, Tyndall Avenue, Bristol BS8 1TL, UK
[6] Australia Telescope National Facility, P.O. Box 76, Epping, NSW 1710, Australia
Received 2009 December 9; accepted 2010 February 11; published 2010 March 24

ABSTRACT

The Sunyaev–Zel'dovich Effect (SZE) has been observed toward six massive galaxy clusters, at redshifts $0.091 \leqslant z \leqslant 0.322$ in the 86–102 GHz band with the Y. T. Lee Array for Microwave Background Anisotropy (AMiBA). We modify an iterative method, based on the isothermal β models, to derive the electron temperature T_e, total mass M_t, gas mass M_g, and integrated Compton Y within r_{2500}, from the AMiBA SZE data. Non-isothermal universal temperature profile (UTP) β models are also considered in this paper. These results are in good agreement with those deduced from other observations. We also investigate the embedded scaling relations, due to the assumptions that have been made in the method we adopted, between these purely SZE-deduced T_e, M_t, M_g, and Y. Our results suggest that cluster properties may be measurable with SZE observations alone. However, the assumptions built into the pure-SZE method bias the results of scaling relation estimations and need further study.

Key words: cosmic background radiation – cosmology: observations – galaxies: clusters: general

1. INTRODUCTION

The Sunyaev–Zel'dovich Effect (SZE) is a useful tool for studies of galaxy clusters. This distortion of the cosmic microwave background (CMB) is caused by the inverse Compton scattering by high-energy electrons as the CMB propagates through the hot plasma of galaxy clusters (Sunyaev & Zel'dovich 1972). The SZE signal is essentially redshift independent, making it particularly useful for determining the evolution of large-scale structure.

For upcoming SZE cluster surveys (Ruhl et al. 2004; Fowler 2004; Kaneko 2006; Ho et al. 2009), it is important to investigate the relations between SZE flux density and other cluster properties such as mass, temperature, and gas fraction. By assuming that the evolution of clusters is dominated by self-similar gravitational processes, we can predict simple power-law relations between integrated Compton Y and other cluster properties (Kaiser 1986). Strong correlations between integrated SZE flux and the mass of clusters are also suggested by numerical simulations (da Silva et al. 2004; Motl et al. 2005; Nagai 2006). These relations imply the possibility of determining the masses and temperatures of clusters, and investigating cluster evolution at high redshift, with SZE observation data alone.

Joy et al. (2001) and Bonamente et al. (2008) demonstrated an iterative approach based on the isothermal β model to estimate the values of electron temperature T_e, total mass M_t, gas mass M_g, and Compton Y from SZE data alone. In this paper, we seek to derive the same cluster properties from the Array for Microwave Background Anisotropy (AMiBA) SZE measurements of six clusters. Due to the limited u–v space sampling, the AMiBA data do not provide useful constraints on the structural parameters, β and r_c, in a full iterative model fitting. Instead, we adopt β and r_c from published X-ray fits and use a Markov Chain Monte Carlo (MCMC) method to determine the cluster properties (T_e, M_t, M_g, and Y). We also estimate these cluster properties from AMiBA data with structural constraints from X-ray data using the non-isothermal universal temperature profile model (Hallman et al. 2007). All quantities are integrated to spherical radius r_{2500} within which the mean overdensity of the cluster is 2500 times the critical density at the cluster's redshift. We then investigate the scaling relations between these cluster properties derived from the SZE data, and identify correlations between those properties that are induced by the iterative method. We note that Huang et al. (2009) investigate the scaling relations between the values of Compton Y from AMiBA SZE data and other cluster properties from X-ray and other data. All results are in good agreement. However, we are concerned that there are embedded relations between the properties we derived using this method. Therefore, we also investigate the embedded scaling relations between SZE-derived properties as well.

We assume the large-scale structure of the universe to be described by a flat ΛCDM model with $\Omega_m = 0.26$, $\Omega_\Lambda = 0.74$, and Hubble constant $H_0 = 72$ km s^{-1} Mpc^{-1}, corresponding to the values obtained using the *WMAP* 5 yr data (Dunkley et al. 2009). All uncertainties quoted are at the 68% confidence level.

2. DETERMINATION OF CLUSTER PROPERTIES

2.1. AMiBA Observation of SZE

AMiBA is a coplanar interferometer (Ho et al. 2009; Chen et al. 2009). During 2007, it was operated with seven close-packed antennas of 60 cm in diameter, giving 21 vector baselines in u–v space and a synthesized resolution of 6′ (Ho et al. 2009).

Table 1
Parameters for Isothermal Spherical β Model

Cluster	z	D_A	Without 100 kpc Cut[a]			With 100 kpc Cut[b]		
			β	r_c	ΔI_0[c]	β	r_c	ΔI_0[c]
		(Mpc)		($''$)	($\times 10^5$ Jy sr^{-1})		($''$)	($\times 10^5$ Jy sr^{-1})
A1689	0.183	621	$0.609^{+0.005}_{-0.005}$	$26.6^{+0.7}_{-0.7}$	-3.13 ± 0.95	$0.686^{+0.010}_{-0.010}$	$48.0^{+1.5}_{-1.7}$	-2.36 ± 0.71
A1995	0.322	948	$0.770^{+0.117}_{-0.063}$	$38.9^{+6.9}_{-4.3}$	-3.30 ± 1.17	$0.923^{+0.021}_{-0.023}$	$50.4^{+1.4}_{-1.5}$	-3.19 ± 1.23
A2142	0.091	340	$0.740^{+0.010}_{-0.010}$	$188.4^{+13.2}_{-13.2}$	-2.09 ± 0.36	...	...	...
A2163	0.202	672	$0.674^{+0.011}_{-0.008}$	$87.5^{+2.5}_{-2.0}$	-3.24 ± 0.56	$0.700^{+0.07}_{-0.07}$ [d]	$78.8^{+0.6}_{-0.6}$ [d]	-3.64 ± 0.61
A2261	0.224	728	$0.516^{+0.014}_{-0.013}$	$15.7^{+1.2}_{-1.1}$	-1.90 ± 0.98	$0.628^{+0.030}_{-0.020}$	$29.2^{+4.8}_{-2.9}$	-2.59 ± 0.90
A2390	0.232	748	$0.600^{+0.060}_{-0.060}$ [e]	$28.0^{+2.8}_{-2.8}$ [e]	-2.04 ± 0.65	$0.58^{+0.058}_{-0.058}$ [e]	$34.4^{+3.4}_{-3.4}$ [e]	-2.85 ± 0.77

Notes.
[a] Reese et al. (2002) for A1689, A1995, A2163, and A2261. Sanderson & Ponman (2003) and Lancaster et al. (2005) for A2142. Allen (2000) for A2390.
[b] Bonamente et al. (2006) for A1689, A1995, A2163, and A2261. Allen et al. (2001) for A2390.
[c] Best-fit values for ΔI_0 with foreground estimation from point sources and CMB (Liu et al. 2010).
[d] β fixed to a fiducial value 0.7 in Bonamente et al. (2006), a 10% error is assumed.
[e] A 10% error is assumed for β and r_c for which the original reference does not give an error estimation.

The antennas are mounted on a 6 m platform (Koch et al. 2009), which we rotate during the observations to provide better u–v coverage. The observations of SZE clusters, the details about the transform of the data into calibrated visibilities, and the estimated cluster profiles are presented in Wu et al. (2009). Further system checks are discussed in Lin et al. (2009) and Nishioka et al. (2009). For other scientific results deduced from AMiBA 2007 observations, please refer to Huang et al. (2009), Liu et al. (2010), Koch et al. (2010), Molnar et al. (2010), and Umetsu et al. (2009).

2.2. Isothermal β Modeling

Because the u–v coverage is incomplete for a single SZE experiment, we can measure neither the accurate profile of a cluster nor its central surface brightness. Therefore, we have chosen to assume an SZE cluster model and thus a surface brightness profile, so that a corresponding template in the u–v space can be fitted to the observed visibilities in order to estimate the underlying model parameters. We consider a spherical isothermal β model (Cavaliere & Fusco-Femiano 1976, 1978), which expresses the electron number density profile as

$$n_e(r) = n_{e0}\left(1 + \frac{r^2}{r_c^2}\right)^{-3\beta/2}, \quad (1)$$

where n_{e0} is the central electron number density, r is the radius from the cluster center, r_c is the core radius, and β is the power-law index.

Traditionally, the SZE is characterized by the Compton-Y parameter, which is defined as the integration along the line of sight (LOS) with given direction,

$$y(\hat{n}) \equiv \int_0^\infty \sigma_T n_e \frac{k_B T_e}{m_e c^2} dl. \quad (2)$$

Compton Y is related to ΔI_{SZE} as

$$\Delta I_{SZE} = I_{CMB} y f(x, T_e) \frac{x e^x}{e^x - 1}, \quad (3)$$

where $x \equiv h\nu/k_B T_{CMB}$, I_{CMB} is the present CMB specific intensity, and $f(x, T_e) = [x \coth(x/2) - 4][1 + \delta_{rel}(x, T_e)]$ (e.g., LaRoque et al. 2006). $\delta_{rel}(x, T_e)$ is a relativistic correction (Challinor & Lasenby 1998), which we take into account to first order in $k_B T_e/m_e c^2$. The relativistic correction becomes significant when the electron temperature exceeds 10 keV, which is the regime of our cluster sample.

One can combine Equations (1)–(3) and integrate along the LOS to obtain the SZE in the apparent radiation intensity as

$$\Delta I_{SZE} = I_0 \left(1 + \theta^2/\theta_c^2\right)^{(1-3\beta)/2}, \quad (4)$$

where θ and θ_c are the angular equivalents of r and r_c, respectively. Because the clusters in our sample are not well resolved by AMiBA, we cannot get a good estimate of I_0, β, and θ_c simultaneously from our data alone. Instead, we use the X-ray-derived values for β and r_c, as summarized in Table 1, and then estimate the central specific intensity I_0 (Liu et al. 2010) by fitting Equation (4) to the calibrated visibilities obtained by Wu et al. (2009). In the analysis, we take into account the contamination from point sources and structures in the primary CMB.

Given the β model described above, we can derive relations between cluster parameters and estimate them using the MCMC method. The parameters to be estimated are the electron temperature T_e, r_{2500}, total mass $M_t \equiv M_t(r_{2500})$, gas mass $M_g \equiv M_g(r_{2500})$, and the integrated Compton $Y \equiv Y(r_{2500})$.

Theoretically, $M_t(r_{2500})$ can be formulated through the hydrostatic equilibrium equation (e.g., Grego et al. 2001; Bonamente et al. 2008):

$$M_t(r_{2500}) = \frac{3\beta k_B T_e}{G\mu m_p} \frac{r_{2500}^3}{r_c^2 + r_{2500}^2}, \quad (5)$$

where G is the gravitational constant and μ is the mean mass per particle of gas in units of the mass of proton, m_p. To calculate μ, we assume that μ takes the value appropriate for clusters with solar metallicity as given by Anders & Grevesse (1989). Here we use the value $\mu = 0.61$. By combining Equation (5) and the definition of r_{2500}, we can obtain r_{2500} as a function of β, T_e, r_c, and redshift z (e.g., Bonamente et al. 2008):

$$r_{2500} = \sqrt{\frac{3\beta k_B T_e}{G\mu m_p} \frac{1}{\frac{4}{3}\pi \rho_c(z) \cdot 2500} - r_c^2}. \quad (6)$$

Table 2
SZE-derived Cluster Properties in Isothermal β Model

Cluster	Without 100 kpc Cut					With 100 kpc Cut				
	r_{2500} ($''$)	$k_B T_e$ (keV)	M_g ($10^{13}\,M_\odot$)	M_t ($10^{14}\,M_\odot$)	Y (10^{-10})	r_{2500} ($''$)	$k_B T_e$ (keV)	M_g ($10^{13}\,M_\odot$)	M_t ($10^{14}\,M_\odot$)	Y (10^{-10})
A1689	209^{+16}_{-19}	$10.4^{+1.6}_{-1.7}$	$4.9^{+1.2}_{-1.2}$	$4.2^{+1.1}_{-1.0}$	$3.2^{+1.5}_{-1.2}$	214^{+16}_{-19}	$10.0^{+1.5}_{-1.6}$	$5.2^{+1.3}_{-1.3}$	$4.5^{+1.2}_{-1.1}$	$3.1^{+1.3}_{-1.2}$
A1995	150^{+13}_{-15}	$12.0^{+1.9}_{-2.2}$	$7.4^{+1.9}_{-2.1}$	$6.4^{+1.7}_{-1.8}$	$1.9^{+1.0}_{-0.8}$	159^{+13}_{-18}	$11.6^{+1.7}_{-2.3}$	$8.5^{+2.4}_{-2.5}$	$7.5^{+2.0}_{-2.3}$	$1.9^{+1.0}_{-0.8}$
A2142	430^{+23}_{-28}	$11.9^{+1.1}_{-1.3}$	$6.6^{+1.1}_{-1.2}$	$5.7^{+1.0}_{-1.0}$	$16.9^{+4.4}_{-4.2}$	...	...	...	...	...
A2163	228^{+14}_{-13}	$15.3^{+1.7}_{-1.5}$	$8.5^{+1.5}_{-1.5}$	$7.2^{+1.4}_{-1.2}$	$7.7^{+2.2}_{-1.9}$	237^{+13}_{-13}	$15.4^{+1.6}_{-1.5}$	$9.5^{+1.6}_{-1.5}$	$8.1^{+1.5}_{-1.3}$	$8.0^{+2.1}_{-1.9}$
A2261	147^{+15}_{-20}	$8.7^{+1.8}_{-2.3}$	$2.7^{+1.0}_{-1.0}$	$2.3^{+0.9}_{-0.9}$	$1.3^{+1.0}_{-0.8}$	172^{+16}_{-15}	$10.0^{+1.8}_{-1.7}$	$4.6^{+1.3}_{-1.2}$	$4.0^{+1.2}_{-1.0}$	$2.2^{+1.1}_{-0.9}$
A2390	156^{+12}_{-15}	$9.2^{+1.3}_{-1.7}$	$3.7^{+0.9}_{-1.0}$	$3.2^{+0.8}_{-0.8}$	$1.6^{+0.7}_{-0.6}$	174^{+13}_{-15}	$11.9^{+1.8}_{-1.9}$	$5.2^{+1.3}_{-1.2}$	$4.4^{+1.1}_{-1.1}$	$3.1^{+1.3}_{-1.2}$

Then $M_g(r_{2500})$ can be expressed, by integrating the $n_e(r)$ in Equation (1), as

$$M_g(r) = 4\pi\mu_e n_{e0} m_p D_A^3 \int_0^{r/D_A} \left(1+\frac{\theta^2}{\theta_c^2}\right)^{-3\beta/2} \theta^2 d\theta, \quad (7)$$

where $\mu_e = 1.17$ is the mean particle mass per electron in units of m_p, D_A is the angular diameter determined by z, and n_{e0} is the central electron density, derived through the equation in LaRoque et al. (2006):

$$n_{e0} = \frac{\Delta T_0 m_e c^2 \Gamma\left(\frac{3}{2}\beta\right)}{f(x, T_e) T_{CMB} \sigma_T k_B T_e D_A \pi^{1/2} \Gamma\left(\frac{3}{2}\beta - \frac{1}{2}\right)\theta_c}, \quad (8)$$

where Γ is the gamma function, ΔT_0 is the SZE temperature change, and T_{CMB} is the present CMB temperature. ΔT_0 is derived as $\Delta T_0/T_{CMB} = (e^x - 1)I_0/xe^x I_{CMB}$.

Finally, with I_0 computed earlier and r_{2500} estimated here, we can integrate the Compton Y out to r_{2500} to yield Y:

$$Y = \frac{2\pi\Delta T_0}{f(x, T_e) T_{CMB}} \int_0^{\theta_{2500}} \left(1+\frac{\theta^2}{\theta_c^2}\right)^{(1-3\beta)/2} \theta d\theta, \quad (9)$$

where $\theta_{2500} = r_{2500}/D_a$ indicates the projected angular size of r_{2500}.

With the formulae as described above, for a set of β, r_c, and z as measured from X-ray observations and I_0 from AMiBA SZE observation, we can arbitrarily assign a "pseudo" electron temperature $T_{e(i)}$, and then determine the pseudo $r_{2500}(T_{e(i)})$, $M_t(T_{e(i)})$, $M_g(T_{e(i)})$, and $Y(T_{e(i)})$. Given $M_t(T_{e(i)})$ and $M_g(T_{e(i)})$, we obtained the pseudo gas fraction $f_{gas}(T_{e(i)}) = M_g(T_{e(i)})/M_t(T_{e(i)})$. Using $f_{gas}(T_{e(i)})$ as a function of $T_{e(i)}$, we applied the MCMC method by varying T_e and ΔI_0 to estimate the likelihood distribution of each cluster property. While estimating the MCMC likelihood, we assume that the likelihoods of ΔI_0 and f_{gas} are independent. The likelihood distributions of ΔI_0 for each cluster are taken from the fitting results of Liu et al. (2010), while the likelihood distribution of f_{gas} is assumed to be Gaussian with mean 0.116 and standard deviation 0.005, which is the ensemble average over 38 clusters observed by *Chandra* and OVRO/BIMA (LaRoque et al. 2006).

In the process, the values of β, r_c, and z are taken from other observational results, which are summarized in Koch et al. (2010) and Table 1. We took the β-model parameters from both *ROSAT* and *Chandra* X-ray results. The *Chandra* results were derived by fitting an isothermal β model to the X-ray data with a central 100 kpc cut. The aim of the cutoff is to exclude the complicated non-gravitational physics (e.g., radiative cooling and feedback mechanisms) in cluster cores. Table 2 summarizes our results derived assuming an isothermal β model. We present the results obtained with isothermal β-model parameters derived with and without 100 kpc cut both here. Figure 1 compares our results with the SZE–X-ray joint results obtained from OVRO/BIMA and *Chandra* data (Bonamente et al. 2008; Morandi et al. 2007). These are in good agreement.

2.3. UTP β Model

The simulation done by Hallman et al. (2007) suggested incompatibility between isothermal β model parameters fitted to X-ray surface brightness profiles and those fitted to SZE profiles. This incompatibility also causes bias in the estimates of Y and M_g. They suggested a non-isothermal β model with a universal temperature profile (UTP). We also considered how the UTP β model changes our estimates of cluster properties in this section.

In the UTP β model, the baryon density profile is the same as Equation (1), and the temperature profile can be written as (Hallman et al. 2007)

$$T_e(r) = \langle T\rangle_{500}\, T_0 \left(1+\left(\frac{r}{\alpha r_{500}}\right)^2\right)^{-\delta}, \quad (10)$$

where $\langle T\rangle_{500}$ indicates the average spectral temperature inside r_{500}. T_0, α, and δ are dimensionless parameters in the universal temperature profile model. δ is the outer slope of the temperature profile, outside of a core with electron temperature $T_{e0} = \langle T\rangle_{500}\, T_0$. This core is of size αr_{500}. The total mass can be obtained by solving the hydrostatic equilibrium equation (Fabricant et al. 1980):

$$M_t(r) = -\frac{k_B r^2}{G\mu m_p}\left(T_e(r)\frac{dn_e(r)}{dr} + n_e(r)\frac{dT_e(r)}{dr}\right). \quad (11)$$

In the isothermal β model, Equation (11) can be reduced into the form of Equation (5). However, in the UTP β model, the derivative of $T_e(r)$ with respect to r in Equation (11) is no longer zero. By applying Equations (1) and (10) in Equation (11), one can obtain

$$M_t(r) = \frac{k_B T_{e0}}{G\mu m_p}\left(\frac{3\beta r^3}{r^2+r_c^2} + \frac{2\delta r^3}{r^2+\alpha^2 r_{500}^2}\right)\left(1+\frac{r^2}{\alpha^2 r_{500}^2}\right)^{-\delta}. \quad (12)$$

By combining Equation (12) and the definition of r_{500}, an analytical solution for r_{500} can be obtained as

$$r_{500} = \sqrt{\frac{(1+\alpha^2)\left(3\beta A - r_c^2\right) + 2\delta A + \sqrt{D}}{2(1+\alpha^2)}}, \quad (13)$$

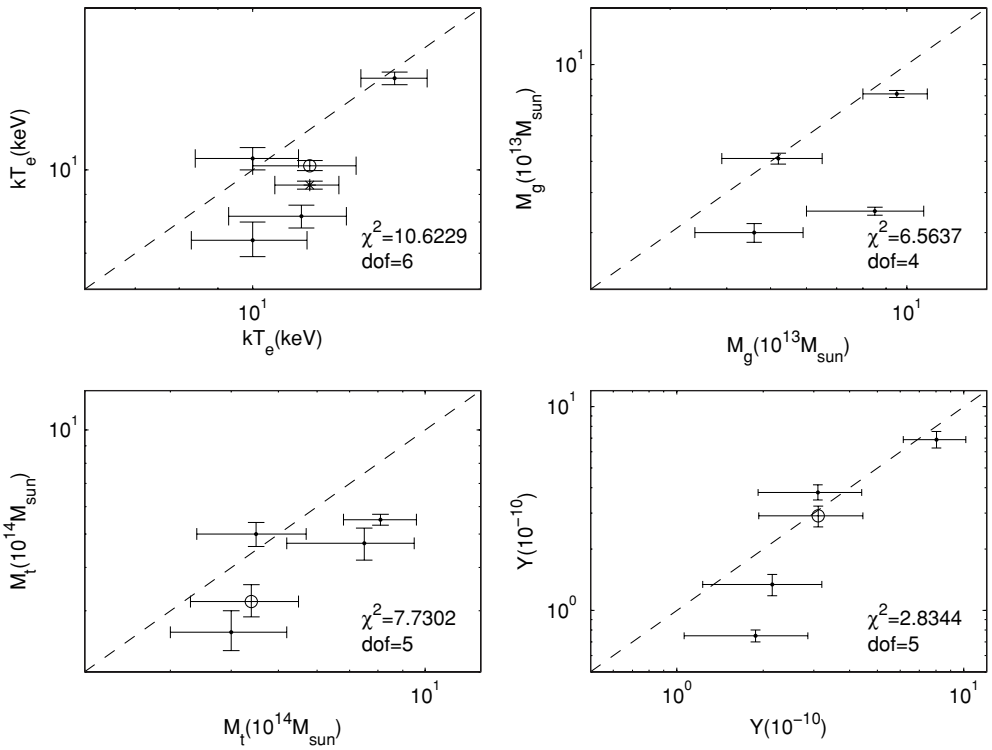

Figure 1. Comparison of T_e (upper left), M_g (upper right), M_t (lower left), and Y (lower right) of clusters derived from AMiBA SZE data based on isothermal β model with 100 kpc cut (x-axis) and those given in the literature (y-axis). All y-axis values are from Bonamente et al. (2008), except for the Y values, which are from Morandi et al. (2007), and those for A2390, which is indicated by a circle with T_e from Benson et al. (2004) and M_t calculated from the data in Benson et al. (2004). The dashed lines indicate $y = x$.

where $A = 3k_B T_{e0}(1+\alpha^{-2})^{-\delta}/(4G\mu m_p \pi \rho_c(z) \cdot 500)$, and $D = [(1+\alpha^2)(3\beta A - r_c^2) + 2\delta A]^2 + 8(1+\alpha^2)\delta A r_c^2$. If $\delta \to 0$ or $\alpha \to \infty$, which indicate the nearly isothermal case, Equation (13) reduces to a form similar to Equation (6).

Using the definition of r_{500}, $M_t(r_{500})$ can be written as

$$M_t(r_{500}) = 500 \cdot \frac{4}{3}\pi r_{500}^3 \rho_c(z). \tag{14}$$

For an arbitrary overdensity Δ, we cannot find an analytical solution for arbitrary r_Δ (i.e., r_{2500}, r_{200}, etc.). However, with the known r_{500}, we can still find the numerical solution for r_Δ easily. We can then solve for $M_t(r_\Delta)$ using Equation (12).

To yield the central electron number density, we consider the formula for the Compton Y resulting from the UTP β model (see the Appendix of Hallman et al. 2007). By setting the projected radius $b = 0$ in Equation (A10) in Hallman et al. (2007), one can obtain

$$n_{e0} = \frac{\Delta T_0 m_e c^2}{f(x, T_e) T_{CMB} \sigma_T k_B \langle T \rangle_{500} T_0 I_{SZ}(0)}, \tag{15}$$

where

$$I_{SZ}(0) = \frac{\pi^{1/2}\Gamma\left(\frac{3}{2}\beta + \delta - \frac{1}{2}\right) F_{2,1}\left(\delta, \frac{1}{2}; \frac{3\beta}{2} + \delta, 1 - \frac{r_c^2}{\alpha^2 r_{500}^2}\right) r_c}{\Gamma\left(\frac{3\beta}{2} + \delta\right)}, \tag{16}$$

and $F_{2,1}$ is Gauss' hypergeometric function. Here, we assume $f(x, T_e) = f(x, \langle T \rangle_{500} T_0)$, and the change of $f(x, T_e)$ due to the change of T_e along LOS is negligible. Actually, by numerical calculation we found that the error in Equation (15) caused by this assumption is less than 1%. Because the UTP β model assumes the electron density profile as same as the isothermal β model, we can rewrite M_g in UTP model by simply applying Equation (15) in Equation (7).

Thus, the integration of the Compton-Y profile, instead of Equation (9), becomes

$$Y = Y_0 \int_0^{\theta_{2500}} \left(1 + \frac{\theta^2}{\theta_c^2}\right)^{(1-3\beta)/2} \left(1 + \frac{\theta^2}{\alpha^2 \theta_{500}^2}\right)^{-\delta} F(\theta) \theta d\theta, \tag{17}$$

where $Y_0 = (2\pi\Delta T_0)/(f T_{CMB} F(0))$ and $F(\theta) = F_{2,1}(\delta, 1/2; 3\beta/2 + \delta, 1 - (r_c^2 + \theta^2)/(\alpha^2 r_{500}^2 + \theta^2))$.

We were not able to constrain the parameters β, r_c, δ, and α of the UTP significantly with our SZE data alone. However, the simulation of Hallman et al. (2007) suggested that there is no significant systematic difference between the values of β and r_c resulting from fitting an isothermal β model to mock X-ray observations and those parameters fitted using the UTP β model. Therefore, we simply assume that the ratio between the isothermal β_{iso} value and UTP β_{UTP} value is 1 ± 0.1 and $r_{c,iso}/r_{c,UTP} = 1 \pm 0.2$ for each cluster. We also assume $\delta = 0.5$, $\alpha = 1$, and $T_0 = 1.3$. Those values are taken from the average of results of Hallman et al. (2007). Then, we fit ΔI_0 to AMiBA SZE observation data with the UTP β-model parameters above by fixing δ, α, and T_0, and treating the likelihood distributions of β_{UTP} and $r_{c,UTP}$ as two independent Gaussian distributions. Finally, we applied the MCMC method, which varies ΔI_0, β, r_c, and $\langle T \rangle_{500}$, to estimate cluster properties with the equations derived from the UTP β model and the data-fitting results.

Table 3 summarizes our results derived with the UTP β model. Figure 2 compares our results with the SZE–X-ray joint results obtained from OVRO/BIMA and *Chandra* data (Bonamente et al. 2008; Morandi et al. 2007). These are also in good

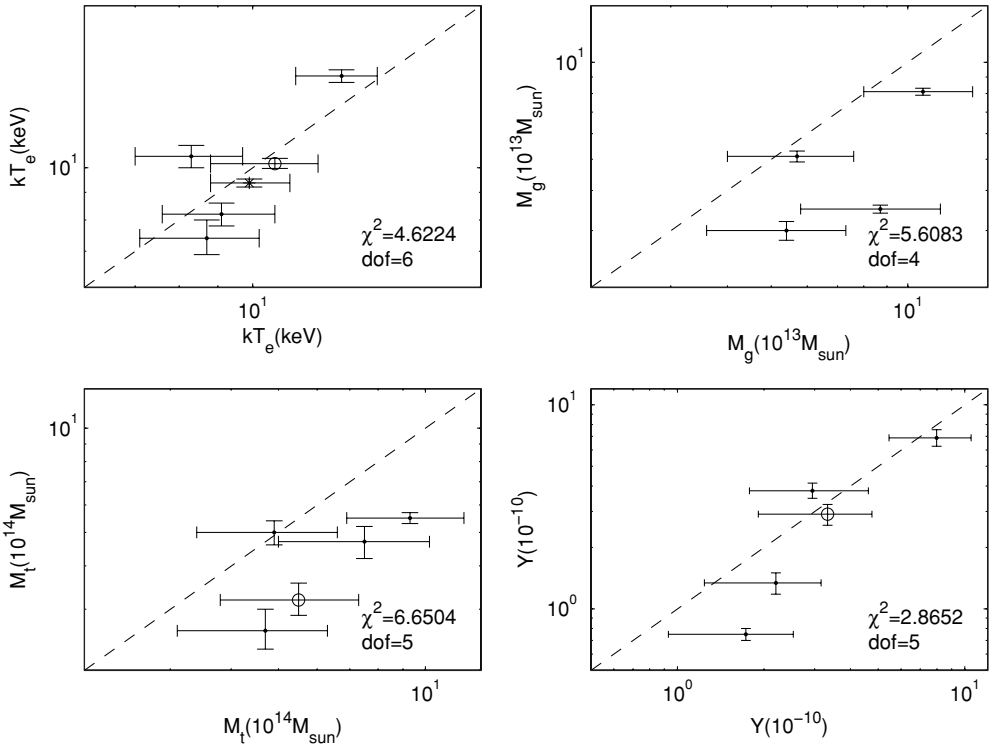

Figure 2. Comparison of T_e (upper left), M_g (upper right), M_t (lower left), and Y (lower right) of clusters derived from AMiBA SZE data based on the UTP β model with 100 kpc cut (x-axis) and those given in the literature (y-axis). All y-axis values are from Bonamente et al. (2008), except for the Y values, which are from Morandi et al. (2007), and those for A2390, which is indicated by a circle with T_e from Benson et al. (2004) and M_t calculated from the data in Benson et al. (2004). The dashed lines indicate $y = x$.

Table 3
SZE-derived Cluster Properties in the UTP β Model

Cluster	Without 100 kpc Cut					With 100 kpc Cut				
	r_{2500} ($''$)	$k_B T_e$[a] (keV)	M_g ($10^{13}\,M_\odot$)	M_t ($10^{14}\,M_\odot$)	Y (10^{-10})	r_{2500} ($''$)	$k_B T_e$[a] (keV)	M_g ($10^{13}\,M_\odot$)	M_t ($10^{14}\,M_\odot$)	Y (10^{-10})
A1689	219^{+23}_{-23}	$8.9^{+1.5}_{-1.6}$	$5.6^{+1.9}_{-1.8}$	$4.8^{+1.7}_{-1.5}$	$3.4^{+1.7}_{-1.5}$	220^{+23}_{-22}	$8.3^{+1.4}_{-1.3}$	$5.7^{+1.9}_{-1.7}$	$4.9^{+1.7}_{-1.5}$	$3.0^{+1.5}_{-1.2}$
A1995	154^{+16}_{-18}	$9.7^{+1.7}_{-1.7}$	$7.6^{+2.8}_{-2.5}$	$6.7^{+2.3}_{-2.3}$	$1.8^{+1.1}_{-0.8}$	161^{+16}_{-20}	$9.1^{+1.6}_{-1.5}$	$8.7^{+3.1}_{-2.9}$	$7.5^{+2.7}_{-2.5}$	$1.9^{+1.0}_{-0.8}$
A2142	458^{+43}_{-49}	$9.9^{+1.1}_{-1.3}$	$7.6^{+2.4}_{-2.3}$	$6.4^{+2.2}_{-1.8}$	$17.0^{+6.5}_{-5.5}$	...	...	...	...	...
A2163	245^{+23}_{-23}	$13.0^{+1.7}_{-1.5}$	$10.1^{+3.0}_{-2.7}$	$8.8^{+2.6}_{-2.4}$	$8.0^{+3.1}_{-2.5}$	251^{+21}_{-24}	$13.1^{+1.5}_{-1.7}$	$10.8^{+3.1}_{-2.8}$	$9.3^{+2.7}_{-2.4}$	$8.3^{+2.9}_{-2.6}$
A2261	160^{+17}_{-22}	$7.9^{+1.5}_{-1.8}$	$3.6^{+1.3}_{-1.4}$	$3.1^{+1.1}_{-1.2}$	$1.5^{+0.9}_{-0.8}$	183^{+20}_{-21}	$8.7^{+1.5}_{-1.6}$	$5.4^{+1.9}_{-1.8}$	$4.7^{+1.6}_{-1.6}$	$2.2^{+1.2}_{-1.0}$
A2390	166^{+17}_{-17}	$8.1^{+1.2}_{-1.4}$	$4.5^{+1.5}_{-1.4}$	$3.9^{+1.3}_{-1.2}$	$1.8^{+0.8}_{-0.7}$	188^{+18}_{-20}	$10.7^{+1.5}_{-1.9}$	$6.3^{+2.1}_{-1.9}$	$5.5^{+1.8}_{-1.7}$	$3.3^{+1.6}_{-1.4}$

Note. [a] The average electron temperature up to r_{500} (i.e., $\langle T \rangle_{500}$ in Equation (10)).

agreement. We find that the electron temperature derived with the UTP β model is in significantly better agreement with the temperatures from *Chandra* X-ray measurements.

3. EMBEDDED SCALING RELATIONS

The self-similar model (Kaiser 1986) predicts simple power-law scaling relations between cluster properties (e.g., Bonamente et al. 2008; Morandi et al. 2007). Motivated by this, people usually investigate the scaling relations between the derived cluster properties from observational data to see whether they are consistent with the self-similar model. However, the method described above is based on the isothermal β model and the UTP β model. Therefore, there could be some embedded relations which agree with the self-similar model predictions between the derived properties. We investigated the embedded relations through both analytical and numerical methods.

3.1. Analytical Formalism and Numerical Analysis

In the isothermal β model, by applying Equation (6) in Equation (5), M_t can be rewritten as

$$M_t = 2500 \cdot \frac{4}{3}\pi\rho_c(z)\left(\frac{3\beta k_B T_e}{G\mu m_p}\frac{1}{2500 \cdot \frac{4}{3}\pi\rho_c(z)} - r_c^2\right)^{\frac{3}{2}}. \quad (18)$$

As we can see, while β is set to be a constant, and $r_{2500}^2 \gg r_c^2$, which implies $3\beta k_B T_e/(G\mu m_p \cdot 2500 \cdot \frac{4}{3}\pi\rho_c(z)) \gg r_c^2$, the relation $M_t \propto T_e^{3/2}$ will be obtained. However, for some of the clusters we considered in this paper, the values of r_{2500}/r_c are only slightly above 2. Therefore, we have to investigate the scaling relation between M_t and T_e by considering $\partial \ln M_t / \partial \ln T_e$.

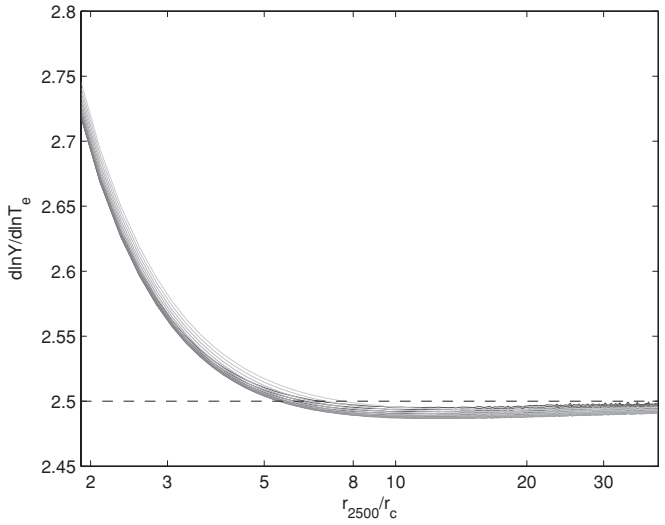

Figure 3. Embedded scaling relation between Y and T_e. The shaded scale indicates different β from 0.5 (the darkest line) to 1.2 (the lightest line). The dashed line indicates the predicted value by the self-similar model.

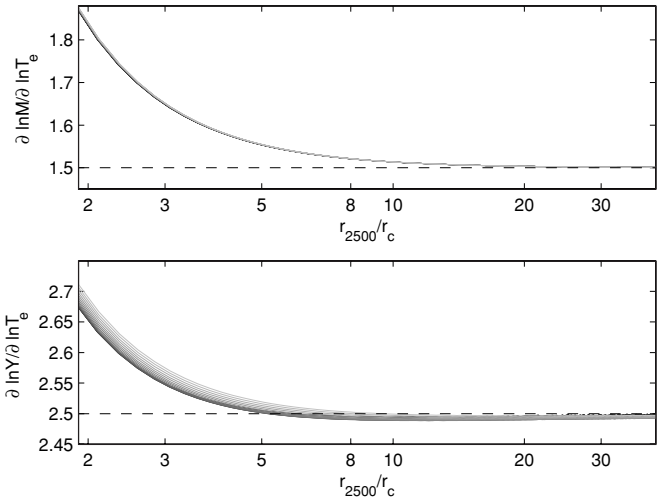

Figure 4. Embedded M_t–T_e (upper panel) and Y–T_e (lower panel) scaling relations in UTP β model. The gray scales indicate different β from 0.5 (the darkest line) to 1.2 (the lightest line). The dashed lines indicate the predicted values by the self-similar model.

By partially differentiating Equation (18) by T_e, and multiplying it by T_e/M_t, we can get

$$\frac{\partial \ln M_t}{\partial \ln T_e} = \frac{3}{2}\frac{\left(r_{2500}^2 + r_c^2\right)}{r_{2500}^2}, \tag{19}$$

which decreases from 1.875 at $r_{2500}/r_c = 2$ to 1.5 as $r_{2500}/r_c \to \infty$. That implies M_t behaves as $M_t \propto T_e^{1.875}$ while $r_{2500}/r_c \approx 2$ and $M_t \propto T_e^{1.5}$, while r_{2500}/r_c approaches infinity. This result shows that there is an embedded M_t–T_e relation consistent with the self-similar model in the method described above.

If we assume that the gas fraction f_{gas} is a constant, the scaling relation between M_g and T_e will be as same as the relation between M_t and T_e.

In order to investigate the relations between integrated Y and the other cluster properties, we consider Equation (9). By combining Equations (6)–(8), one can obtain

$$\Delta T_0 = \frac{M_g(r_{2500}) f(x, T_e) T_{CMB} \sigma_T k_B T_e \Gamma\left(\frac{3}{2}\beta - \frac{1}{2}\right)\theta_c}{4\pi^{1/2}\mu_e m_p D_A^2 m_e c^2 \Gamma\left(\frac{3}{2}\beta\right) \int_0^{\theta_{2500}} \left(1 + \frac{\theta^2}{\theta_c^2}\right)^{-3\beta/2} \theta^2 d\theta}. \tag{20}$$

We then combine Equations (9) and (20) and obtain

$$Y = \frac{\pi^{1/2} M_g(r_{2500}) \sigma_T k_B T_e}{2\mu_e m_p m_e c^2 D_A^2} g(\theta_{2500}, \theta_c, \beta), \tag{21}$$

where

$$g(\theta_{2500}, \theta_c, \beta) = \frac{\Gamma\left(\frac{3}{2}\beta - \frac{1}{2}\right)\theta_c \int_0^{\theta_{2500}} \left(1 + \frac{\theta^2}{\theta_c^2}\right)^{(1-3\beta)/2} \theta d\theta}{\Gamma\left(\frac{3}{2}\beta\right) \int_0^{\theta_{2500}} \left(1 + \frac{\theta^2}{\theta_c^2}\right)^{-3\beta/2} \theta^2 d\theta} \tag{22}$$

is a dimensionless function of θ_{2500}, θ_c, and β.

We also calculated $\partial \ln Y/\partial \ln T_e$ to investigate the behavior of Y when T_e varies (see Figure 3). As we can see in Figure 3, $\partial \ln Y/\partial \ln T_e$ varies between 2.45 and 2.75, while $r_{2500}/r_c > 2.0$ and $0.5 \leqslant \beta \leqslant 1.2$. We also noticed that $\partial \ln Y/\partial \ln T_e$ approaches 2.5 as r_{2500}/r_c approaches infinity. This result indicates that behavior similar to the self-similar model is built into scaling relation studies based solely on SZE data.

The effect of varying β is investigated. If we consider power-law scaling relation

$$Q = 10^A X^B \tag{23}$$

between M_t and T_e with M_t written as Equation (18), one can find that changing the value of β will only affect the normalization factor A. In other words, if we change β to β', A will be changed to $A' = A + B \log_{10}(\beta'/\beta)$.

In the Y–T_e relation, β will affect the scaling power B as shown in Figure 3. B varies within a range of only 0.04, while $0.5 \leqslant \beta \leqslant 1.2$.

Considering the UTP β model, we undertook a similar analysis of the embedded scaling relation. The results, which are similar with those obtained with the isothermal β model, are shown in Figure 4.

3.2. Calculation of Scaling Relations

Here, we investigate the Y–T_e, Y–M_t, and Y–M_g scaling relations for the quantities derived above. We also study the M_t–T_e scaling relation with the M_t from AMiBA SZE data and the T_e from X-ray data (Bonamente et al. 2008; Morandi et al. 2007).

For a pair of cluster properties Q–X, we consider the power-law scaling relation (Equation (23)). To estimate A and B, we perform a maximum likelihood analysis in the log–log plane. For the M_t–T_e relation, because M_t and T_e are independent measurements from different observational data, we can simply perform linear minimum-χ^2 analysis to estimate A and B (Press et al. 1992; Benson et al. 2004). On the other hand, for the SZE-derived properties, because they are correlated and so are their likelihoods (i.e., $L(Q, X) \neq L(Q)L(X)$, as manifested by the colored areas in Figure 5), we cannot apply χ^2 analysis. Instead, we use a Monte Carlo method by randomly choosing one MCMC iteration from each cluster many times. With each set of iterations, we derived a pair of A_i and B_i using linear regression method. Finally, we estimate the likelihood distribution of A and B using the distribution of $\{A_i\}$ and $\{B_i\}$. The results are presented in Table 4 and Figures 5 and 6. However, as we discussed in Section 3.1, the scaling relations between SZE-derived properties should be interpreted as a test of embedded scaling relations rather than estimations of the true scaling

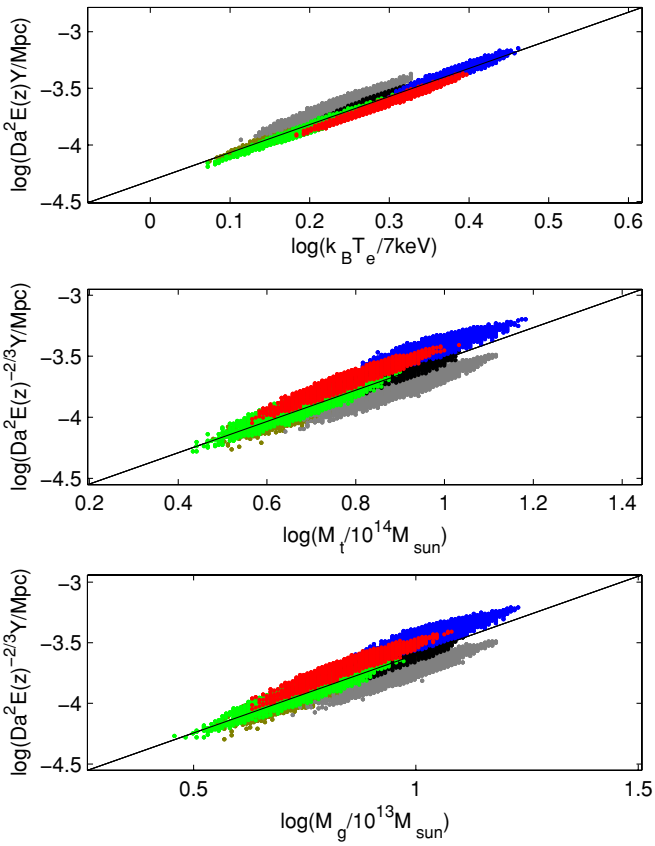

Figure 5. Scaling relations of Y–T_e (upper), Y–M_g (middle), and Y–M_t (lower) based on the AMiBA SZE-derived results. Gray areas indicate the 68% confidence regions for the parameter pairs of each cluster. Solid lines are the best fits as in Table 4.

Table 4
Scaling Relations of SZE-derived Cluster Properties

Scaling Relations	A	B	$B_{\rm thy}$
$D_A^2 E(z) Y,\ T$	$-4.32^{+0.07}_{-0.06}$	$2.48^{+0.20}_{-0.22}$	2.50
$D_A^2 E(z)^{-2/3} Y,\ M_t$	$-4.80^{+0.21}_{-0.21}$	$1.28^{+0.27}_{-0.23}$	1.67
$D_A^2 E(z)^{-2/3} Y,\ M_g$	$-4.89^{+0.22}_{-0.22}$	$1.29^{+0.28}_{-0.25}$	1.67
$E(z) M_t,\ T$	$0.66^{+0.11}_{-0.12}$	$0.95^{+0.66}_{-0.60}$	1.50

Notes. All cluster properties used in the analysis are based on the AMiBA SZE data (see Section 2), except for the T in the M–T relation, where the T is from Bonamente et al. (2008) for A1689, A1995, A2163, A2261, and from Morandi et al. (2007) for A2390. The units of T, $D_A^2 Y$, M_t, and M_g are 7 keV, Mpc^2, $10^{14}\ M_\odot$, and $10^{13}\ M_\odot$, respectively. The last column $B_{\rm thy}$ indicates the theoretical values predicted by the self-similar model. In the first column, $E^2(z) \equiv \Omega_M (1+z)^3 + (1-\Omega_M-\Omega_\Lambda)(1+z)^2 + \Omega_\Lambda$.

relations. On the other hand, the M_t–T_e relation compared M_t and T_e from different experiments. Therefore, we can regard it as a test of the scaling relation prediction.

4. DISCUSSIONS AND CONCLUSION

We derived the cluster properties, including T_e, r_{2500}, M_t, M_g, and Y, for six massive galaxy clusters ($M_t(r_{2500}) > 2\times10^{14}\ M_\odot$) mainly based on the AMiBA SZE data. These results are in good agreement with those obtained solely from the OVRO/BIMA SZE data, and those from the joint SZE–X-ray analysis of *Chandra*–OVRO/BIMA data. In comparison, the SZE–X-ray joint analysis gives smaller error bars than the pure SZE

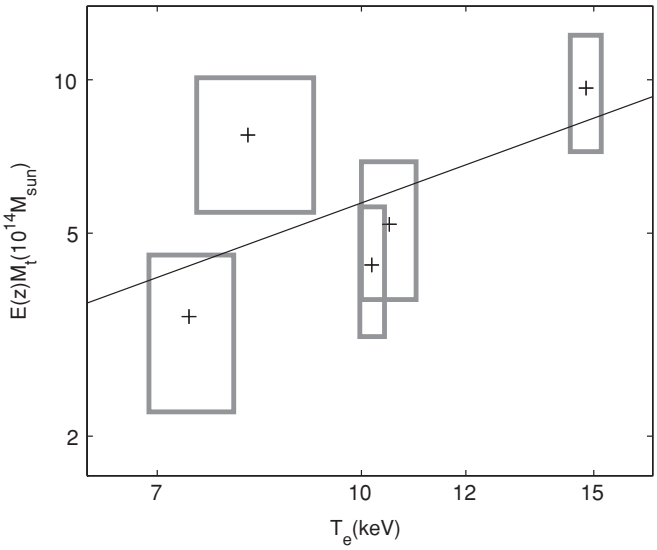

Figure 6. M_t–T_e scaling relation between the X-ray-measured T_e (Bonamente et al. 2008; Morandi et al. 2007) and the AMiBA-derived M_t. The boxes indicate the 1σ errors for each cluster. The solid line is the best fit as in Table 4.

results, because currently the uncertainty in the measurement of the SZE flux is still large. On the other hand, in our current SZE-based analysis, due to the insufficient u–v coverage of the seven-element AMiBA we still need to use X-ray parameters for the cluster model, i.e., the β and θ_c for the β model. However, Nord et al. (2009) have deduced β and θ_c from an APEX SZE observation alone recently. For AMiBA, the situation will be improved when it expands to its 13 element configuration with 1.2 m antennas (AMiBA13; Ho et al. 2009), and thus much stronger constraints on the cluster properties than current AMiBA results are expected. Furthermore, with about three times higher angular solution, we should be able to estimate β and θ_c from our SZE data with AMiBA13 and make our analysis purely SZE-based (Ho et al. 2009; Molnar et al. 2010). Nevertheless, the techniques of using SZE data solely to estimate cluster properties are still important, because many upcoming SZE surveys will observe SZE clusters for which no X-ray data are available (Ruhl et al. 2004; Fowler 2004; Kaneko 2006; Ho et al. 2009), especially for those at high redshifts.

Hallman et al. (2007) suggested that adopting the UTP β model for SZE data on galaxy clusters will reduce the overestimation of the integrated Compton Y_{500} and gas mass. However, the Y_{2500} values we obtained with the UTP model are not smaller than those obtained with the isothermal model. The $M_g(r_{2500})$ values deduced using the UTP model are even larger than those deduced using the isothermal model.

For the case of integrated Compton Y, when we compare Y_{500} deduced using the UTP model $Y_{500,\rm UTP}$, and those deduced using the isothermal model $Y_{500,\rm iso}$, we find that the $Y_{500,\rm UTP}$ are smaller than $Y_{500,\rm iso}$, as predicted by Hallman et al. (2007). The reason is that the Compton-Y profile predicted using the UTP β model will decrease more quickly than the profile predicted by the isothermal β model, with increasing radius. Therefore, the ratio $Y_{\Delta,\rm UTP}/Y_{\Delta,\rm iso}$ will decrease as Δ decreases.

We also noticed that the electron temperature values obtained with the isothermal model are significantly higher than the temperatures deduced from X-ray data for most clusters we considered. The temperatures of clusters obtained using the UTP model are lower than those obtained with the isothermal model and thus are in better agreement with those deduced from X-ray

data. Therefore, in the UTP model, with similar Y_{2500} and lower temperature, we should get larger M_g.

The electron temperatures derived using the UTP β model are in better agreement with X-ray observation results than those derived using the isothermal β model. This result implies that the UTP β model may provide better estimates of the electron temperature when we can use only the β-model parameters from X-ray observation. However, we noticed that the UTP β model produced larger error bars than the isothermal β model did. These increased errors are based on the uncertainties of β and r_c which we insert by hand. On the other hand, because we treat β and r_c as independent parameters in this work, the uncertainty could be overestimated due to the degeneracy between these two parameters. If we can access to the likelihood distributions of β and r_c of the UTP β model derived from observation, the error bars might be reduced significantly.

There is a concern that the scaling relations among the purely SZE-derived cluster properties may be implicitly embedded in the formalism we used here. In this paper, we also investigate for the first time the embedded scaling relations between the SZE-derived cluster properties. Our analytical and numerical analyses both suggest that there are embedded scaling relations between SZE-derived cluster properties, with both the isothermal model and the UTP model, while we fix β. The embedded Y–T and M–T scaling relations are close to the predictions of the self-similar model. The results imply that the assumptions built in the pure-SZE method significantly affect the scaling relation between the SZE-derived properties. Therefore, we should treat those scaling relations carefully.

Our results suggest the possibility of measuring cluster parameters with SZE observation alone. The agreement between our results and those from the literature provides not only confidence for our project but also supports our understanding of galaxy clusters. The upcoming expanded AMiBA with higher sensitivity and better resolution will significantly improve the constraints on these cluster properties. In addition, an improved determination of the u–v space structure of the clusters directly from AMiBA will make it possible to measure the properties of clusters which currently do not have good X-ray data. The ability to estimate cluster properties based on SZE data will improve the study of mass distribution at high redshifts. On the other hand, the fact that the assumptions of cluster mass and temperature profiles significantly bias the estimations of scaling relations should be also noticed and treated carefully.

We thank the Ministry of Education, the National Science Council (NSC), and the Academia Sinica, Taiwan, for their funding and supporting of AMiBA project. Y.W.L. thanks the AMiBA team for their guiding, supporting, hard working, and helpful discussions. We are grateful for computing support from the National Center for High-Performance Computing, Taiwan. This work is also supported by National Center for Theoretical Science, and Center for Theoretical Sciences, National Taiwan University for J.-H.P.W. Support from the STFC for M. Birkinshaw is also acknowledged.

REFERENCES

Allen, S. W. 2000, MNRAS, 315, 269
Allen, S. W., Ettori, S., & Fabian, A. C. 2001, MNRAS, 324, 877
Anders, E., & Grevesse, N. 1989, Geochim. Cosmochim. Acta, 53, 197
Benson, B. A., Church, S. E., Ade, P. A. R., Bock, J. J., Ganga, K. M., Henson, C. N., & Thompson, K. L. 2004, ApJ, 617, 829
Bonamente, M., Joy, M., LaRoque, S., Carlstrom, J., Nagai, D., & Marrone, D. 2008, ApJ, 675, 106
Bonamente, M., Joy, M., LaRoque, S., Carlstrom, J., Reese, E. D., & Dawson, K. S. 2006, ApJ, 647, 25
Cavaliere, A., & Fusco-Femiano, R. 1976, A&A, 49, 137
Cavaliere, A., & Fusco-Femiano, R. 1978, A&A, 70, 677
Challinor, A. D., & Lasenby, A. N. 1998, ApJ, 499, 1
Chen, M. T., et al. 2009, ApJ, 694, 1664
da Silva, A. C., Kay, S. T., Liddle, A. R., & Thomas, P. A. 2004, MNRAS, 348, 1401
Dunkley, J., et al. 2009, ApJS, 180, 306
Fabricant, D., Lecar, M., & Gorenstein, P. 1980, ApJ, 241, 552
Fowler, J. W. 2004, Proc. SPIE, 5498, 1
Grego, L., Carlstrom, J. E., Reese, E. D., Holder, G. P., Holzapfel, W. L., Joy, M. K., Mohr, J. J., & Patel, S. 2001, ApJ, 552, 2
Hallman, E. J., Burns, J. O., Motl, P. M., & Norman, M. L. 2007, ApJ, 665, 911
Ho, P. T. P., et al. 2009, ApJ, 694, 1610
Huang, C.-W. L., et al. 2010, ApJ, in press (arXiv:0911.3232v1)
Joy, M., et al. 2001, ApJ, 551, L1
Kaiser, N. 1986, MNRAS, 222, 323
Kaneko, T. 2006, Proc. SPIE, 6267, 62673R
Koch, P. M., et al. 2009, ApJ, 694, 1670
Koch, P. M., et al. 2010, ApJ, submitted
Lancaster, K., et al. 2005, MNRAS, 359, 16
LaRoque, S. J., Bonamente, M., Carlstrom, J. E., Joy, M. K., Nagai, D., Reese, E. D., & Dawson, K. S. 2006, ApJ, 652, 917
Lin, K. Y., et al. 2009, ApJ, 694, 1629
Liu, G. C., et al. 2010, ApJ, submitted
Molnar, S. M., et al. 2010, submitted
Morandi, A., Ettori, S., & Moscardini, L. 2007, MNRAS, 379, 518
Motl, P. M., Hallman, E. J., Burns, J. O., & Norman, M. L. 2005, ApJ, 623, L63
Nagai, D. 2006, ApJ, 650, 538
Nishioka, H., et al. 2009, ApJ, 694, 1637
Nord, M., et al. 2009, A&A, 506, 623
Press, W. H., Teukolsky, S. A., Vetterling, W. T., & Flannery, B. P. 1992, Numerical Recipes in C: The Art of Scientific Computing (2nd ed.; Cambridge: Cambridge Univ. Press)
Reese, E. D., Carlstrom, J. E., Joy, M., Mohr, J. J., Grego, L., & Holzapfel, W. L. 2002, ApJ, 581, 53
Ruhl, J. E., et al. 2004, Proc. SPIE, 5498, 11
Sanderson, A. J. R., & Ponman, T. J. 2003, MNRAS, 345, 1241
Sunyaev, R. A., & Zel'dovich, Ya. B. 1972, Comments Astrophys. Space Phys., 4, 173
Umetsu, K., et al. 2009, ApJ, 694, 1643
Wu, J. H. P., et al. 2009, ApJ, 694, 1619